

Low Frequency Air-Bone Gap in Meniere's Disease: Relationship With Magnetic Resonance Imaging Features of Endolymphatic Hydrops

Irumee Pai,^{1,2,4} and Steve Connor^{2,3,4}

Objectives: The appearance of low-frequency air-bone gaps (LFABGs) in Meniere's disease (MD) is a recognized but relatively unexplored phenomenon. Two theories have been proposed to explain their etiology: increased perilymphatic pressure resulting in either reduced stapedial mobility or dampened transmission of acoustic energy, and direct contact between the dilated saccule and the stapes footplate. The aim of this study was to evaluate these two hypotheses by comparing delayed post-gadolinium magnetic resonance imaging (MRI) features of two groups of patients with unilateral definite MD, those with and without LFABGs.

Design: This retrospective case-control study was conducted at a tertiary otolaryngology unit in the United Kingdom. The study included 35 patients who satisfied the 2015 Barany criteria for unilateral definite MD. The cohort was divided into two groups, those with LFABGs (LFABG+ group) and those without (LFABG- group), according to the pure-tone audiometry performed within 6 months of MRI. Alternative potential causes for the LFABGs were excluded on the basis of otologic history, otoscopy, tympanometry, and/or imaging. Using a 4-hr delayed post-gadolinium 3-dimensional fluid-attenuated inversion recovery sequence, two observers evaluated the severity of cochlear and vestibular endolymphatic hydrops (EH) and the presence of vestibular endolymphatic space contacting the oval window (VESCO). The air and bone conduction thresholds, ABGs and MRI features were compared between the LFABG+ and LFABG- groups. Where any of the variables were found to be significantly associated with the presence of ABGs, further analysis was performed to determine whether or not they were independent predictors. Continuous variables were compared using the independent *t* test if normally distributed, and the Mann-Whitney U test or Kruskal-Wallis test if not normally distributed. Categorical variables were compared with Pearson's Chi-squared test or Fishers/Fisher-Freeman-Halton exact tests.

Results: There were 10 patients in the LFABG+ group (28.6%) and 25 patients in the LFABG- group (71.4%). The mean ABGs in the symptomatic ear at 500 Hz, 1 kHz, and 2 kHz were 15.1 dB \pm 6.4, 10.5 dB \pm 9.0, and 4.0 dB \pm 7.7, respectively, in the LFABG+ group and 2.0 \pm 5.8, 2.4 \pm 4.4, and -0.8 \pm 4.7 dB in the LFABG- group. The differences in ABGs between the two groups were statistically significant at all three test frequencies ($p < 0.001$ at 500 Hz, $p = 0.007$ at 1 kHz, and $p = 0.041$ at 2 kHz). The presence of ABGs was significantly associated with both the grade of vestibular EH ($p = 0.049$) and VESCO ($p = 0.009$). Further analysis showed a statistically significant association between the grade of vestibular EH

and VESCO ($p = 0.007$), and only VESCO was an independent variable associated with the presence of LFABGs ($p = 0.045$).

Conclusions: The study findings add to the existing body of evidence that LFABGs are a true audiological finding in MD and allow us to propose a mechanism. Analysis of delayed gadolinium-enhanced MRI suggests that direct contact between the distended saccule and the inner surface of the stapes footplate is the more likely underlying pathophysiological mechanism for this audiometric phenomenon.

Key words: Air-bone gaps, Conductive, Endolymphatic hydrops, Hearing loss, Magnetic resonance imaging, Meniere's disease.

(Ear & Hearing 2022;43;1678–1686)

INTRODUCTION

Meniere's disease (MD) is a disorder of the inner ear that is characterized by spontaneous episodes of vertigo associated with fluctuating hearing loss, tinnitus, and aural fullness. In the absence of definitive objective tests, the diagnosis of MD is based on clinical symptoms and audiometry. Whilst histopathological studies proposed endolymphatic hydrops (EH) as the underlying pathophysiological mechanism in MD many decades ago (Frayssé et al. 1980), the recent advances in magnetic resonance imaging (MRI) have enabled in vivo visualization of the endolymphatic and perilymphatic compartments of the inner ear, thus allowing evaluation of the relationship between imaging features of EH and clinical manifestation of MD (Conte et al. 2018a; Lopez-Escamez & Attyé 2019).

The pattern of hearing loss most characteristic of MD is fluctuating low- to medium-frequency sensorineural hearing loss (SNHL; Lopez-Escamez et al. 2015). One aspect of hearing loss associated with MD that has received relatively little attention is the phenomenon of low-frequency air-bone gaps (LFABGs) in the absence of middle ear pathology, which has been reported to occur in 14 to 33% of MD patients (Muchnik et al. 1989; Yetişer & Kertmen 2007; Lee et al. 2014). Muchnik et al. (1989) proposed two hypotheses to account for the presence of LFABGs: either increased perilymphatic pressure dampening the stapedial mobility or dilatation of the saccule applying a direct force to the stapes footplate. A single study investigating the underlying pathophysiological mechanism for LFABGs by Sugimoto et al. (2018) showed that the average ABG at 250 Hz was significantly larger in ears with EH that reached the stapes footplate on MRI than in those without. Based on their findings, the authors proposed that the appearance of LFABGs suggested progression of EH and that it could be a useful indicator for disease activity. More recently, Kobayashi et al. (2020) reported that ears with significant EH showed significantly higher hearing thresholds, ABGs and higher absorbance values on wideband acoustic immittance at low frequencies compared

¹Department of Otolaryngology, Guy's and St. Thomas' Hospitals, London, United Kingdom; ²School of Biomedical Engineering & Imaging Sciences Clinical Academic Group, King's College London, London, United Kingdom; and ³Department of Radiology, Guy's and St. Thomas' Hospitals, London, United Kingdom; ⁴These authors contributed equally to the study design, data collection and analysis, and preparation and review of the final manuscript.

Copyright © 2022 The Authors. Ear & Hearing is published on behalf of the American Auditory Society, by Wolters Kluwer Health, Inc. This is an open-access article distributed under the terms of the Creative Commons Attribution-Non Commercial-No Derivatives License 4.0 (CCBY-NC-ND), where it is permissible to download and share the work provided it is properly cited. The work cannot be changed in any way or used commercially without permission from the journal.

with those with nonsignificant EH, and postulated that reduced transmission of acoustic energy to the inner may be responsible for the LFABGs.

Based on the two aforementioned hypotheses, the present study aimed to compare both the overall degree of vestibular EH and the contact of endolymphatic structures with the oval window on MRI in unilateral MD patients with and without LFABGs.

MATERIALS AND METHODS

The study underwent local institutional review and was approved. The Strengthening the Reporting of Observational Studies in Epidemiology (STROBE) guidelines for case-control studies were followed.

Study Subjects

The indications for hydrops MRI in our institution are as follows:

1. Unilateral MD, when invasive therapies (e.g., intratympanic injection) are being considered
2. MD with bilateral aural symptoms
3. Episodic vertigo equivocal for MD, where an alternative or overlapping diagnosis is being considered
4. Sudden-onset or fluctuating SNHL
5. Fluctuating aural fullness and tinnitus

The present study included all adult patients (aged 16 years or older) with unilateral definite MD, who underwent MRI for EH at our institution between September 2017 and November 2020. The clinical diagnosis of definite MD was based on the 2015 Barany criteria (Lopez-Escamez et al. 2015). Exclusion criteria included the presence of another potential cause that could account for ABGs (e.g., abnormal otoscopy or tympanometry, history of middle ear disease/surgery), and no availability of pure-tone audiometry (PTA) within 6 months of MRI. Clinical data collection included gender, affected ear, duration of MD, and the time interval between PTA and imaging.

Audiometric Criteria

PTA and tympanometry were performed according to the British Society of Audiology recommended procedures (British Society of Audiology 2018a, b). Audiometric data collection for the purpose of this study included air conduction (AC) thresholds at 250 Hz, 500 Hz, 1 kHz, 2 kHz, and 4 kHz and bone conduction (BC) thresholds at 500 Hz, 1 kHz, and 2 kHz. The cohort was divided into two groups, those with LFABGs on at least one audiogram within 6 months before or after MRI (“LFABG+ group”) and those without LFABGs on any of the audiograms within this time frame (“LFABG– group”), based on the difference between the AC and BC thresholds at 500 Hz, 1 kHz, and 2 kHz. The definition of an ABG used in this study was adapted from the criteria described by Muchnik et al. (1989):

1. ABG of at least 20 dB at one or more frequencies
- or
2. ABG of at least 15 dB at one frequency and at least 10 dB at another frequency

Where multiple audiograms of the same nature of hearing loss were available within the 6-month time frame either before

or after MRI, the one performed closest to the scan date was used in the analysis.

Imaging Acquisition, Processing, and Analysis

MRI was performed on a 3 Tesla Siemens Magnetom Skyra scanner, 3.5 to 4.5 hr after the intravenous administration of double-dose gadolinium-based contrast agent (0.2 mmol/kg). An isotropic (0.7 mm voxel size) high-resolution 3-dimensional fluid-attenuated inversion recovery (“3-dimensional fluid-attenuated inversion recovery [3D FLAIR]”) sequence (repetition time = 6000 msec, echo time = 180 msec, inversion time = 2000 msec, number of excitations = 1, flip angle = 180°, echo train length = 27, pixel spacing = 0.7 mm, slice thickness = 0.7 mm, 256 × 240 matrix) was obtained using a 32-channel head coil. This 4-hr delayed postgadolinium 3D FLAIR sequences demonstrated the endolymphatic space as nonenhancing (low signal), the perilymphatic space as enhancing (high signal) and the adjacent bone of the otic capsule as low signal. A high-resolution isotropic (0.3 mm voxel size) T2-weighted sampling perfection with application optimized contrasts using different flip angle evolution (“SPACE”) sequence was also acquired to help delineate the combined endolymphatic and perilymphatic spaces which are both demonstrated as high signal.

Processing and analysis were performed on the institutional Picture Archiving and Communication System database (Sectra AB, Sweden). The two observers (both with 4 years of imaging experience in interpreting MRI of EH) evaluated the MRI studies by consensus and blinded both to the laterality of the clinical MD diagnosis and to the hearing profile.

To grade the vestibular endolymphatic space enlargement, an axial reformat of the isotropic 3D FLAIR sequence was angled to a plane encompassing the posterior limb of lateral semicircular canal and the modiolus, and this was used to define the largest cross section through the vestibule (Fig. 1). The T2 SPACE sequence was reformatted with an identical obliquity for reference. The image window level and width were set according to a standard algorithm. The area of the vestibular endolymphatic space (comprising utricle, saccule, and any semicircular canal ampullae) was compared with that of the combined vestibular endolymphatic and perilymphatic space. When it was difficult to define the border of the endolymphatic space at its interface with the low signal bone, this was aided by correlating with the T2 SPACE sequence (Fig. 2). A four-point semiquantitative grading system for the vestibular endolymphatic space enlargement was derived from previous studies (Nakashima et al. 2009b; Baráth et al. 2014; Fig. 3):

1. Grade 0: vestibular endolymphatic space <33% combined vestibular endolymphatic and perilymphatic space
2. Grade 1: vestibular endolymphatic space 33 to 50% combined vestibular endolymphatic and perilymphatic space
3. Grade 2: vestibular endolymphatic space >50% combined vestibular endolymphatic and perilymphatic space but not completely replacing the perilymphatic space
4. Grade 3: vestibular endolymphatic space completely replacing the perilymphatic space

The assessment of vestibular endolymphatic space contacting the oval window (VESCO) on the 3D FLAIR sequence was reproduced from that previously described by Conte et al. (2018b). This was demonstrated by the presence of nonenhancing

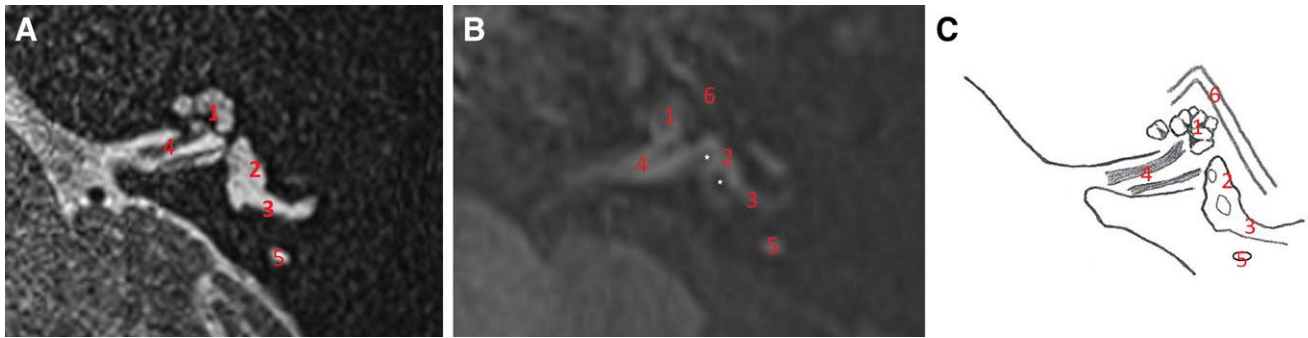


Fig. 1. Normal appearances of the inner ear anatomy illustrated on axial sections in an asymptomatic ear. A, T2 SPACE axial image and B, Delayed post gadolinium 3D FLAIR image. The images depict the vestibular area at its maximum and are angled from the posterior limb of the lateral semicircular canal to the mid-modiolar cochlea. (1) mid-modiolar cochlea, (2) vestibule, (3) lateral semicircular canal posterior limb, (4) internal auditory meatus, (5) posterior semicircular canal, (6) horizontal portion of facial nerve canal. The endolymphatic structures (*) are shown with the utricle posteriorly and the saccule anteriorly. C, Schematic diagram of the delayed post gadolinium 3D FLAIR image (B). 3D FLAIR indicates 3-dimensional fluid-attenuated inversion recovery; SPACE, sampling perfection with application optimized contrasts using different flip angle evolution.

endolymphatic space bulging into the pars inferioris to replace the enhancing perilymphatic space behind the stapes footplate. Both a para-axial double oblique reformat (angled parallel to the lateral semi-circular canal in axial, coronal, and sagittal planes; Fig. 4) and a para-sagittal double oblique reformat (angled parallel to the superior semicircular canal in coronal and axial planes) were obtained (Fig. 5). VESCO was recorded if the vestibular endolymphatic space contacted the oval window on both reformatted images (Figs. 4 and 6).

The degree of cochlear EH was also recorded on a three-point Likert scale using the Nakashima grading system (Nakashima et al. 2009b):

1. Grade 0: no hydrops
2. Grade 1: mild hydrops (Reissner's membrane displaced)
3. Grade 2: marked hydrops (size of the cochlear duct exceeding the area of the scala vestibuli)

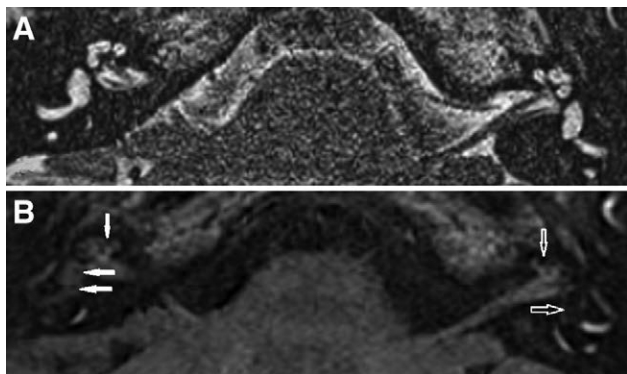


Fig. 2. Appearances of endolymphatic hydrops in the left ear of a patient with unilateral left sided Meniere's disease and an asymptomatic right ear. A, T2 SPACE axial image does not discriminate between the endolymphatic and perilymphatic spaces; however, it outlines the periphery of the perilymphatic space. B, 3D FLAIR image demonstrates the endolymphatic structures as low signal and the enhancing perilymphatic structures as high signal. On the right side, filled horizontal arrows demonstrate the normal saccule (anteriorly) and utricle (posteriorly) whilst a vertical filled arrow shows (asymptomatic) grade 1 cochlear hydrops. On the left side, open horizontal arrow shows the enlarged fused utricle and saccule with a peripheral rim of perilymphatic enhancement with grade 2 vestibular hydrops, whereas a vertical filled arrow indicates grade 2 cochlear hydrops. 3D FLAIR indicates 3-dimensional fluid-attenuated inversion recovery; SPACE, sampling perfection with application optimized contrasts using different flip angle evolution.

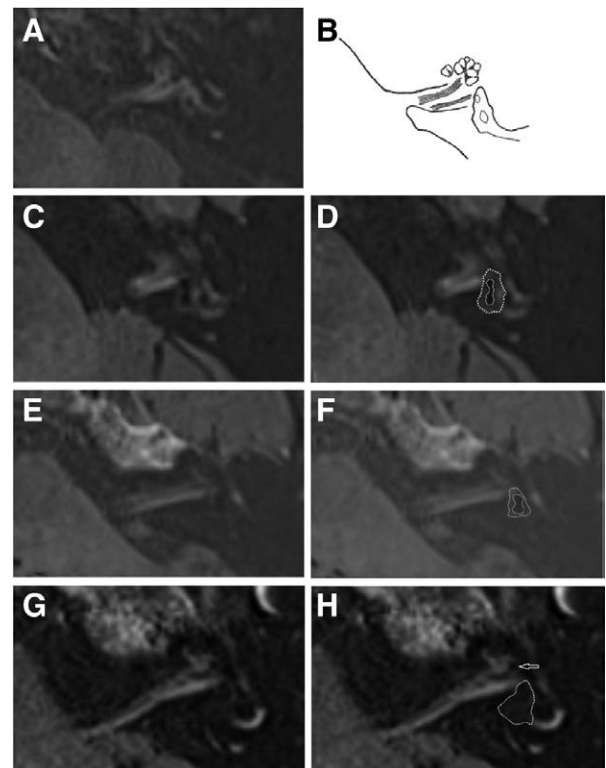


Fig. 3. Delayed postgadolinium 3D FLAIR images demonstrating the grading of vestibular hydrops in symptomatic Meniere's disease ears on the identical axial sections through the vestibule. Grade 0 (A, B) corresponds to normal appearances of the vestibular endolymphatic structures as also depicted in Figure 1. The nonenhancing endolymphatic space is $<33\%$ of the sum of the endolymphatic and perilymphatic spaces. Grade 1 vestibular hydrops (C, D) is demonstrated as the nonenhancing endolymphatic space being $>33\%$ but $<50\%$ of the sum of the endolymphatic and perilymphatic spaces. Grade 2 vestibular hydrops (E, F) is demonstrated as the nonenhancing endolymphatic space being $>50\%$ of the sum of the endolymphatic and perilymphatic spaces but not completely replacing the vestibular perilymphatic enhancement. Grade 3 vestibular hydrops (G, H) is demonstrated as the endolymphatic space completely replacing the vestibular perilymphatic enhancement. (D, F, and H) correspond to (C, E, and G) but with the endolymphatic space (continuous line) and the perilymphatic space (dotted line) outlined. Note in (G) and (H), the perilymphatic space is replaced by endolymphatic space and the T2w sequences are used to guide the outline of the perilymph. The enlarged cochlear duct (arrow) is also indicated in (H). 3D FLAIR indicates 3-dimensional fluid-attenuated inversion recovery.

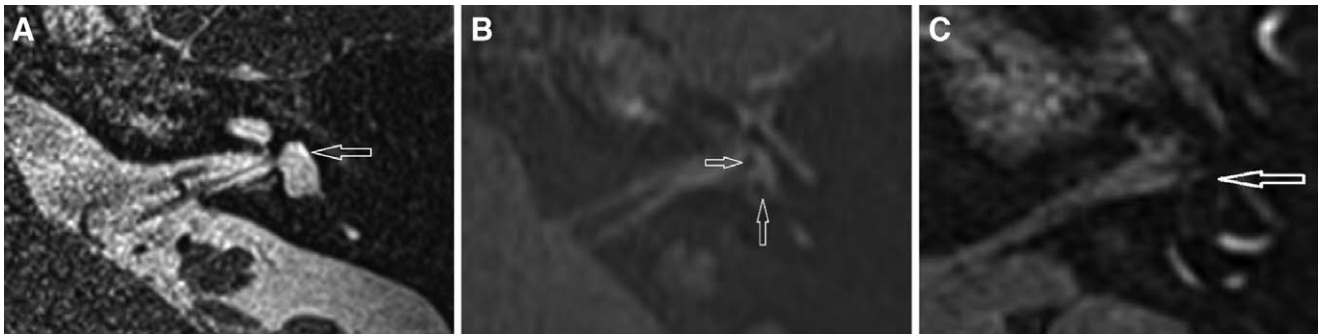


Fig. 4. Evaluation of VESCO on axial sections through the oval window within the inferior third of the vestibule and parallel to the lateral semicircular canal. In an asymptomatic ear without VESCO (A) T2 SPACE with the horizontal arrow indicating the location of the oval window and (B) delayed postgadolinium 3D FLAIR with the enhancing perilymph contacting the oval window. There is no encroachment from the nonenhancing saccule (horizontal arrow in B) or utricle (vertical arrow in B). C, In a patient with left-sided Meniere's disease and VESCO, the fused saccule and utricle contacts the oval window (horizontal arrow). 3D FLAIR indicates 3-dimensional fluid-attenuated inversion recovery; SPACE, sampling perfection with application optimized contrasts using different flip angle evolution; VESCO, vestibular endolymphatic space contacting the oval window.

In addition, other MRI features that could potentially account for the presence of an ABG were assessed, namely superior semicircular canal dehiscence, middle ear/mastoid effusion, and large vestibular aqueduct syndrome. Finally, computed tomography (CT) studies were also reviewed where available to exclude potential causes for ABGs, such as otosclerosis and ossicular chain discontinuity.

Statistical Analysis

Statistical analysis was performed using SPSS (version 27; IBM, Armonk, New York), with a p value of <0.05 being considered statistically significant.

The AC and BC thresholds, ABGs, vestibular and cochlear EH grades, and the presence of VESCO were compared between the LFABG+ and LFABG- groups. Where any of the variables were found to be significantly associated with the presence of ABGs, further analysis was performed to determine whether or not they were independent predictors. Continuous variables were compared using the independent t test if normally distributed, and the Mann-Whitney U test or Kruskal-Wallis test if not normally distributed. Categorical variables were compared with Pearson's Chi-squared test or Fishers/Fisher-Freeman-Halton exact tests.

RESULTS

Demographic and Audiological Data

A total of 38 patients with unilateral definite MD had undergone delayed gadolinium-enhanced 3D FLAIR MRI between September 2017 and November 2020 at our institution. Of these, 3 patients did not have PTA within 6 months of imaging and were excluded from analysis. The study therefore included 35 patients, with a female preponderance (female:male = 22:13). The mean age at imaging for the whole cohort was 51.2 ± 13.5 (SD) years (range 26.5 to 79.3). The right ear ($n = 17/35$) and left ear ($n = 18/35$) were equally affected. Otoscopy and tympanometry were documented to be normal in all cases.

Based on the audiometric criteria, there were 10 patients in the LFABG+ group ($n = 10/35$, 28.6%) and 25 patients in the LFABG- group ($n = 25/35$, 71.4%). The mean ABGs in the symptomatic ear at 500 Hz, 1 kHz, and 2 kHz were $15.1 \text{ dB} \pm 6.4$, $10.5 \text{ dB} \pm 9.0$, and $4.0 \text{ dB} \pm 7.7$, respectively in the LFABG+ group and $2.0 \pm 5.8 \text{ dB}$, $2.4 \pm 4.4 \text{ dB}$ and $-0.8 \pm 4.7 \text{ dB}$ in the LFABG- group. The differences in ABGs between the two groups were statistically significant at all three test frequencies ($p < 0.001$ at 500 Hz, $p = 0.007$ at 1 kHz, and $p = 0.041$ at 2 kHz). All but one patient in the LFABG+ group had at least one audiogram subsequent to the one used in the study,

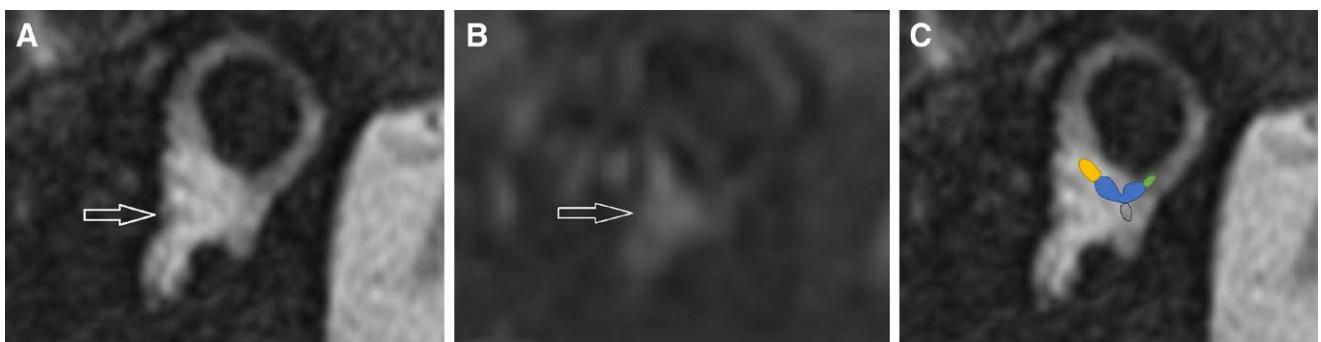


Fig. 5. Evaluation of VESCO on oblique sagittal reconstruction parallel to the superior semicircular canal. In an asymptomatic ear without VESCO (A) T2 SPACE and (B) delayed postgadolinium 3D FLAIR show the enhancing perilymph contacting the oval window (arrow in A and B) with no encroachment from the utricle or its ampullary extensions. C, T2 SPACE image with diagrammatic overlay to indicate normal vestibular endolymphatic space in the oblique sagittal image used to evaluate for VESCO. Blue: utricle; yellow: lateral semicircular canal and ampullary extension; green: superior semicircular canal duct; gray: posterior semicircular canal ampullary extension (saccule is not demonstrated in this plane). 3D FLAIR indicates 3-dimensional fluid-attenuated inversion recovery; SPACE, sampling perfection with application optimized contrasts using different flip angle evolution; VESCO, vestibular endolymphatic space contacting the oval window.

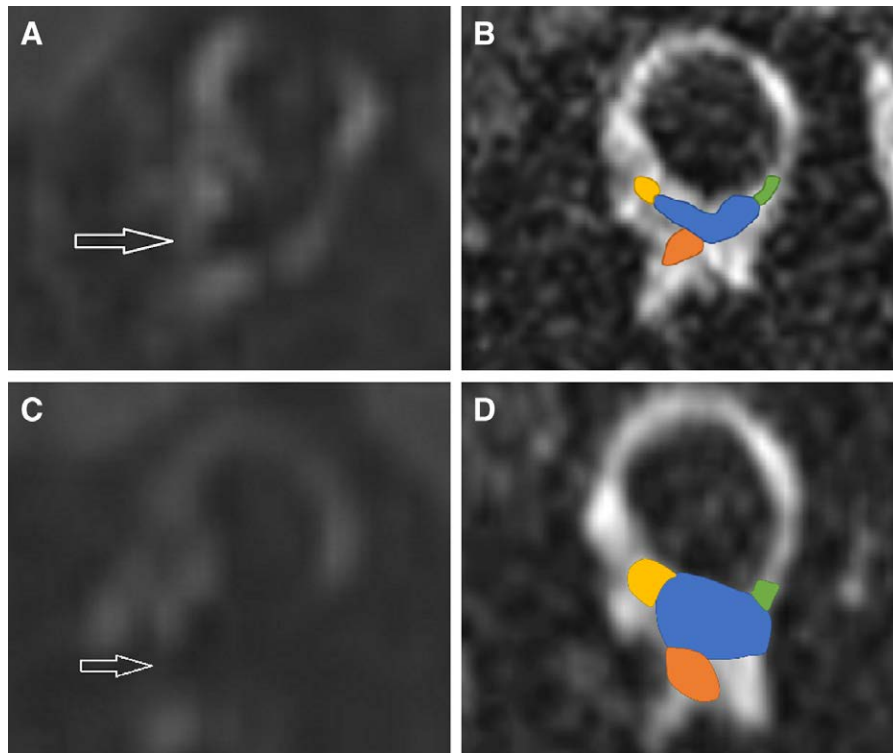


Fig. 6. VESCO on oblique sagittal reconstructions parallel to the superior semicircular canal. A, Delayed postgadolinium 3D FLAIR images. B, T2 SPACE image with diagrammatic overlay to indicate the endolymphatic structures, in a symptomatic Meniere's disease ear with grade 2 vestibular hydrops but without VESCO. The enhancing perilymph is seen adjacent to the oval window (arrow in A) without contact from endolymphatic structures. C, Delayed postgadolinium 3D FLAIR images. D, T2 SPACE image with diagrammatic overlay to indicate the endolymphatic structures, in a symptomatic Meniere's disease ear with grade 3 vestibular hydrops and with VESCO. The enhancing perilymph is effaced at the oval window due to contact by the endolymphatic structures demonstrated (open arrow in C). Blue: utricle; yellow: lateral semicircular canal ampullary extension; green: superior semicircular canal duct; orange: saccule. 3D FLAIR indicates 3-dimensional fluid-attenuated inversion recovery; SPACE, sampling perfection with application optimized contrasts using different flip angle evolution; VESCO, vestibular endolymphatic space contacting the oval window.

on which ABGs were no longer evident. Four patients, including the one patient who had persistent LFABGs, had additional CT which did not show any potential cause that could account

TABLE 1. Demographic and clinical data for LFABG+ and LFABG- groups

	LFABG+	LFABG-	<i>p</i>
Mean age (yrs) ± SD	49.9 ± 7.9	51.7 ± 15.0	0.600
Gender (female:male)	4:6	18:7	-
Median duration of MD (yrs) [interquartile range]	9 [2.5–13.8]	5 [2.4–13.8]	0.380
Median interval PTA-MRI (mo)	2.5 [1.4–3.2]	1.4 [1.3–1.9]	0.152
Symptomatic ear			
AC thresholds (dB HL)			
250 Hz	63.0 ± 15.7	57.0 ± 18.1	0.365
500 Hz	64.5 ± 10.9	57.4 ± 16.5	0.221
1 kHz	60.5 ± 19.2	53.8 ± 20.8	0.386
2 kHz	48.5 ± 21.4	48.8 ± 22.8	0.877
BC thresholds (dB HL)			
500 Hz	49.0 ± 9.4	55.2 ± 15.8	0.363
1 kHz	50.0 ± 16.8	51.6 ± 21.1	0.832
2 kHz	48.5 ± 20.1	48.8 ± 22.4	0.971
ABG (dB)			
500 Hz	15.5 ± 6.4	2.0 ± 5.8	<0.001
1 kHz	10.5 ± 9.0	2.4 ± 4.4	0.006
2 kHz	4.0 ± 7.7	-0.8 ± 4.7	0.041

Bold values indicate statistically significant.

AC, air conduction; BC, bone conduction; LFABG, low-frequency air-bone gap; MD, Meniere's disease; MRI, magnetic resonance imaging; PTA, pure-tone audiometry.

for the conductive component of the hearing loss. None of the patients in either group had an ABG that met the audiometric criteria used in this study in the asymptomatic contralateral ear.

There was no statistically significant difference between the two groups in the mean age, the time intervals between onset of MD and imaging and between PTA and imaging, or the mean AC and BC thresholds at any of the test frequencies. The demographic and clinic data for the two groups are summarized in Table 1.

Imaging Analysis

The imaging quality of the 4-hr delayed gadolinium 3D FLAIR sequence was of diagnostic quality in all 35 cases. There was no case of superior semicircular canal dehiscence or large vestibular aqueduct syndrome in either group. One patient in the LFABG- group had patchy opacification in the peripheral mastoid air cells in the contralateral ear, but there was no air-bone gap at any of the test frequencies (0, 5, and 5 dB at 500 Hz, 1 kHz, and 2 kHz, respectively) and the tympanometry was normal.

The details of the imaging analysis are summarized in Table 2. The presence of LFABGs was significantly associated with both the grade of vestibular EH ($p = 0.049$) and VESCO ($p = 0.009$), but not with the grade of cochlear EH ($p = 0.575$).

The significant associations between LFABGs, vestibular EH and VESCO were in turn explored by examining (1) the relationship between vestibular EH and VESCO, (2) the influence of vestibular EH on the association between LFABGs and

TABLE 2. Comparison of imaging findings between LFABG+ and LFABG– groups

	LFABG+	LFABG–	<i>p</i>
Symptomatic ipsilateral ear			
Vestibular EH grade			0.049
Grade 0	0% (0/10)	12% (3/25)	
Grade 1	0% (0/10)	36% (9/25)	
Grade 2	60% (6/10)	36% (9/25)	
Grade 3	40% (4/10)	16% (4/25)	
VESCO	90% (9/10)	40% (10/25)	0.009
Cochlear EH grade			0.58
Grade 0	0% (0/10)	8% (2/25)	
Grade 1	0% (0/10)	12% (3/25)	
Grade 2	100% (10/10)	80% (20/25)	
Asymptomatic contralateral ear			
Vestibular EH grade			0.08
Grade 0	80% (8/10)	100% (25/25)	
Grade 1	20% (2/10)	0% (0/25)	
Grade 2	0% (0/10)	0% (0/25)	
Grade 3	0% (0/10)	0% (0/25)	
VESCO	0% (0/10)	0% (0/25)	NA
Cochlear EH grade			0.31
Grade 0	40% (4/10)	60% (15/25)	
Grade 1	60% (6/10)	32% (8/25)	
Grade 2	0% (0/10)	8% (2/25)	

Bold values indicate statistically significant.

EH, endolymphatic hydrops; LFABG, low-frequency air-bone gap; NA, not applicable; VESCO, vestibular endolymphatic space contacting the oval window.

VESCO, (3) the influence of VESCO status on the association between LFABGs and vestibular EH. Further analysis showed a statistically significant association between the grade of vestibular EH and VESCO ($p = 0.007$). When subgroup analysis was performed on those with grade 2 or 3 vestibular EH, the presence of LFABGs was shown to be significantly associated with VESCO ($p = 0.045$). In contrast, when the cohort was subdivided by the VESCO status into VESCO positive (VESCO+) and VESCO negative (VESCO–) groups, no association was found between the presence of LFABGs and the grade of vestibular EH in either subgroup ($p = 0.650$ in the VESCO+ group, $p = 0.562$ in the VESCO– group). This indicates that vestibular EH grade is associated with LFABGs through its association with VESCO but is not an independent variable. The details of the subgroup analyses are summarized in Tables 3 and 4.

No case of VESCO was found in the asymptomatic control ear in any of the patients. When the study cohort was divided by the VESCO status in the symptomatic ear, there were 19 patients in the VESCO+ group ($n = 19/35$, 54%) and 16 patients in the VESCO– group ($n = 16/35$, 46%). Although LFABGs

TABLE 3. Association between VESCO and LFABGs when stratified by vestibular EH grading

	LFABG+	LFABG–	<i>p</i>
Vestibular EH grades 0/1			0.16
VESCO+	0	2	
VESCO–	0	10	
Vestibular EH grades 2/3			0.045
VESCO+	9	8	
VESCO–	1	5	

Bold value indicates statistically significant.

EH, endolymphatic hydrops; LFABG, low-frequency air-bone gap; VESCO, vestibular endolymphatic space contacting the oval window.

TABLE 4. Association between vestibular EH grading and LFABGs when stratified by VESCO status

	LFABG+	LFABG–	<i>p</i>
VESCO+			0.65
Vestibular EH grades 0/1	0	2	
Vestibular EH grades 2/3	9	8	
VESCO–			0.56
Vestibular EH grades 0/1	0	10	
Vestibular EH grades 2/3	1	5	

EH, endolymphatic hydrops; LFABG, low-frequency air-bone gap; VESCO, vestibular endolymphatic space contacting the oval window.

were present in only 9 of the 19 patients (47%) in the VESCO+ group, they were absent in 15 of 16 patients (94%) in the VESCO– group. The sensitivity, specificity, positive predictive value, and negative predictive value of LFABGs and VESCO are summarized in Table 5.

DISCUSSION

The appearance of LFABGs in MD is a recognized but relatively unexplored phenomenon. Two theories have been proposed to explain their etiology: direct contact between the dilated saccule and the stapes footplate and increased perilymphatic pressure resulting in either reduced stapedial mobility or dampened acoustic energy transmission to the inner ear. In this study, we aimed to explore these two hypotheses by comparing the imaging features of two groups of unilateral definite MD patients, those with and those without LFABGs, on 4-hr delayed postgadolinium 3D FLAIR MRI. Whilst the absence of a rim of perilymphatic gadolinium enhancement medial to the oval window was interpreted as direct contact between the endolymphatic compartment and the stapes footplate, the severity of vestibular EH was evaluated in lieu of the perilymphatic pressure, since there is no way of directly measuring the pressure within the inner ear in the clinical setting. The initial findings appeared to indicate that the presence of LFABGs was associated both with the severity of vestibular EH and with VESCO. Further analysis showed that there was a significant association between these two variables, and it was only VESCO that was independently associated with the presence of LFABGs.

The appearance of LFABGs in MD was first observed by Holmgren in 1964, who considered them to be an artifact due to harmonic distortion generated by the BC receiver (Holmgren 1964). Subsequently, however, a number of studies described the finding as a true audiological phenomenon in MD. In one of the earliest studies that specifically examined this subject, Muchnik et al. (1989) found fluctuating ABGs in a third of MD cases and postulated that it was caused by pathophysiological

TABLE 5. Diagnostic values of LFABGs and VESCO in unilateral MD

	LFABGs for MD (%)	VESCO for LFABGs (%)
Sensitivity	29	90
Specificity	100	60
PPV	100	47
NPV	58	94

LFABG, low-frequency air-bone gap; MD, Meniere's disease; NPV, negative predictive value; PPV, positive predictive value; VESCO, vestibular endolymphatic space contacting the oval window.

changes in inner ear fluid dynamics, endolymphatic or perilymphatic hypertension, rather than by middle ear dysfunction. In a longitudinal follow-up study by Yetişer and Kertmen (2007), which reported a similar incidence of 28.4%, a higher rate of conductive involvement was observed in patients who have had a recent episode of vertigo. The authors proposed either saccular hydrops extending to the inner surface of the stapes footplate or increased hydrostatic pressure preventing stapes vibratory movement as the potential underlying pathophysiological mechanism. In a more recent study, Lee et al. (2014) found that the number of vertigo spells and hearing thresholds were significantly higher during the period of LFABG development and proposed that it likely reflected the aggravation of the EH in the cochlear and vestibular compartments.

One of the great challenges associated with MD is the lack of well-established, objective tests that can provide *in vivo* information about the disease process. In this regard, the recent advances in imaging of EH may be considered as a highly significant development. Since high-resolution T2-weighted MRI sequences of the inner ear structures cannot distinguish between the endolymphatic and perilymphatic compartments, the role of imaging in MD used to be limited to exclusion of other diagnoses. It was first discovered in animal studies that gadolinium accumulated in the perilymph but not in the endolymphatic compartment due to the presence of impermeable tight junctions (Counter et al. 1999; Niyazov et al. 2001). This knowledge, together with other advances in MRI technologies and techniques, has enabled *in vivo* depiction of EH and increasing application in clinical settings (Nakashima et al. 2007; Naganawa et al. 2008b, 2010; Baráth et al. 2014; Naganawa & Nakashima 2014; Attyé et al. 2017). In human studies, intravenous administration of gadolinium has largely superseded the initial approaches of intratympanic gadolinium, which is less invasive, allows simultaneous assessment of both ears and requires a 4-hr, rather than 24-hr, delay. Currently, the most widely utilized MRI sequences for imaging of EH are 3D FLAIR, as used in the present study, or 3D Real-Inversion Recovery sequences (Naganawa et al. 2008a, 2019; Nakashima et al. 2009a; Baráth et al. 2014; Attyé et al. 2017).

The first study to investigate the relationship between imaging features of EH on MRI and ABGs was by Sugimoto et al. (2018). In their study, the authors divided a cohort of patients with significant vestibular and cochlear EH into two groups, those with vestibular EH adjacent to the stapes footplate and those without, and compared their AC thresholds, BC thresholds and ABGs. The study found that there was a statistically significant difference in ABG at 250 Hz (8.7 ± 8.1 dB in EH with adjacency versus 3.0 ± 7.9 dB in EH without adjacency), and EH adjacency to the stapes footplate was associated with significantly higher average BC thresholds at all frequencies. In addition, ears with significant cochlear and vestibular EH adjacent to the stapes footplate had more MD with long duration than those with no adjacency.

It should be noted that there are two substantial differences between the present study and the study by Sugimoto et al. (2018) in terms of methodology. First, whilst the previous study included all cases of significant EH of various etiologies, including delayed EH, fluctuating hearing loss, acute SNHL, chronic hearing loss, unspecified vertigo, ear fullness as well as MD, we strictly limited it to those who met the 2015 Barany criteria for unilateral definite MD. Second, Sugimoto et al. essentially

compared the audiometric profiles of all significant EH cases divided into two groups according to the presence or absence of EH adjacent to the stapes footplate, whereas our study aimed to specifically seek the underlying etiology for the presence of LFABG in patients with definite MD through imaging. Furthermore, Sugimoto et al. found a statistically significant difference in ABG between adjacent EH and nonadjacent EH groups at 250 Hz, but it could potentially be argued that, as an audiological finding, the significance of the mean ABG (8.7 ± 8.1 dB) observed in the adjacent EH group should be interpreted with some caution. Nonetheless, both studies appear to confirm a link between LFABGs and saccular EH contacting the stapes footplate.

Comparison of the outcomes and findings from different studies is not a straightforward task due to the differences in audiometric definitions used, standard audiological practice, and study methodology. For instance, Lee et al. (2014) calculated the 3-frequency average at 250 Hz, 500 Hz, and 1 kHz and defined LFABGs as a mean difference between AC and BC thresholds equal to or greater than 10 dBHL and present at 2 or more contiguous frequencies. In contrast, Muchnik et al. (1989), from whose study our audiometric criteria were derived, used 20 dB or greater at one frequency or 15 dB at one frequency and 10 dB at another as definitions of ABGs. In the studies by Yetişer & Kertmen (2007) and Sugimoto et al. (2018), ABGs are calculated as the differences between AC and BC thresholds, without a specific definition of what constitutes a significant ABG. Another factor to bear in mind is the long-standing debate regarding the accuracy of BC testing at various frequencies, particularly at 250 Hz (Shipton et al. 1980; Coles et al. 1991; Lightfoot 2000), which is therefore not recommended for BC testing in the guidelines by the British Society of Audiology and American Academy of Audiology. Moreover, given the differences in the standard audiological practice, it may not be possible to accurately replicate study methodologies from other centers. However, despite the differences in methodology and variable incident rates reported (14 to 33%), it seems irrefutable now that LFABGs are one of the possible audiometric features of MD.

Our study findings suggest that that the presence of VESCO has high sensitivity and negative predictive value (90 and 94%, respectively) but low specificity and positive predictive value (60 and 47%, respectively) for LFABGs. In view of the imaging interpretation method used, the most likely explanation is the low signal to noise ratio of hydrops MRI and the consequent failure to detect a very thin rim of gadolinium-containing endolymphatic space under the stapes footplate, resulting in false positive VESCO. On the other hand, detection of a bright rim, an indicator of a lack of contact between the endolymphatic compartment and the stapes footplate, appears to correlate very well with the absence of LFABGs. Although there is no feasible way at present to truly validate this imaging interpretation, it is interesting to review the study outcomes in conjunction with a histological study conducted more than three decades ago by Okuno and Sando (1987), in which saccular EH was found to extend laterally to touch the footplate in 17 out of 22 temporal bones from individuals with MD.

The authors acknowledge that the present study has a number of limitations. First, it is not possible to fully account for fluctuations in LFABGs and potential consequent variations in the degree of EH and/or presence of VESCO on MRI (Sone et al. 2010). To mitigate for this uncertainty as far as possible, study

inclusion was restricted to those who had PTA within 6 months of imaging, and the median interval between PTA and MRI was 2.5 months in the LFABG+ group and 1.4 months in the LFABG− group. Ideally, imaging would have been repeated to correlate spontaneous resolution of LFABGs with any changes on MRI; however, due to the requirement for repeated intravenous gadolinium, such practice is currently not considered in our institution. Second, it is appreciated that MRI parameters such as inversion time may influence the degree of hydrops depicted (Bykowski et al. 2015). However, in the current case-controlled study, the same MRI sequence was applied to both groups and hence this technical aspect is unlikely to have influenced the results. Third, other specific causes of conductive hearing loss such as otospongiosis and ossicular discontinuity were excluded on CT in only four patients in the LFABG+ group. Nonetheless, it should be noted that the LFABGs spontaneously disappeared on subsequent audiograms in all patients but one (who had a normal CT), which makes such potential etiologies unlikely. Fourth, since in our institution unilateral MD patients generally undergo hydrops imaging when being considered for invasive therapies, it is possible that the findings from this study may not necessarily be applicable to all patients with MD; that said, there does not appear to be a convincing or logical reason as to why an alternative pathophysiological mechanism would be at work in MD patients with LFABGs who are in remission. Finally, our use of the grade of vestibular EH to test the hypothesis that increased perilymphatic pressure may dampen the stapedial mobility or acoustic energy transmission could be criticized. Although a popular mechanical supposition postulates that the distension of the membranous labyrinth in EH is related to endolymphatic hypertension, the empirical evidence for an actual increase in pressure during active disease is weak, and there are no data to support transmission of increased pressure to the perilymphatic space (Andrews & Strelhoff 1995). However, this does not detract from our principle finding of an association between VESCO and LFABGs.

CONCLUSION

In our cohort of unilateral definite MD patients, the incidence of LFABGs was 28.6%, adding to the existing body of evidence that they are a true audiological finding in MD. Analysis of delayed gadolinium-enhanced MRI suggests that direct contact between the distended saccule and the inner surface of the stapes footplate is the more likely underlying pathophysiological mechanism for this audiometric phenomenon.

ACKNOWLEDGMENTS

The authors have no conflicts of interest to disclose.

Address for correspondence: Irumee Pai, St. Thomas' Hearing Implant Centre, 2nd floor Lambeth Wing, St. Thomas' Hospital, Westminster Bridge Road, London SE1 7EH, United Kingdom. E-mail: irumee.pai@kcl.ac.uk

Received July 9, 2021; accepted March 30, 2022; published online ahead of print May 18, 2022.

REFERENCES

Andrews, J. C., & Strelhoff, D. (1995). Modulation of inner ear pressure in experimental endolymphatic hydrops. *Otolaryngol Head Neck Surg*, *112*, 78–83.

- Attyé, A., Eliezer, M., Boudiaf, N., Tropres, I., Chechin, D., Scherber, S., Dumas, G., Krainik, A. (2017). MRI of endolymphatic hydrops in patients with Meniere's disease: A case-controlled study with a simplified classification based on saccular morphology. *Eur Radiol*, *27*, 3138–3146.
- Baráth, K., Schuknecht, B., Naldi, A. M., Schrepfer, T., Bockisch, C. J., Hegemann, S. C. (2014). Detection and grading of endolymphatic hydrops in Ménière disease using MR imaging. *AJNR Am J Neuroradiol*, *35*, 1387–1392.
- British Society of Audiology. (2018a). Recommended procedure: pure-tone air-conduction and bone-conduction threshold audiometry with and without masking. <https://www.thebsa.org.uk/resources/>
- British Society of Audiology. (2018b). Recommended procedure: tympanometry. <https://www.thebsa.org.uk/resources/>
- Bykowski, J., Harris, J. P., Miller, M., Du, J., Mafee, M. F. (2015). Intratympanic contrast in the evaluation of meniere disease: Understanding the limits. *AJNR Am J Neuroradiol*, *36*, 1326–1332.
- Coles, R. R., Lutman, M. E., Robinson, D. W. (1991). The limited accuracy of bone-conduction audiometry: Its significance in medicolegal assessments. *J Laryngol Otol*, *105*, 518–521.
- Conte, G., Lo Russo, F. M., Calloni, S. F., Sina, C., Barozzi, S., Di Berardino, F., Scola, E., Palumbo, G., Zanetti, D., Triulzi, F. M. (2018a). MR imaging of endolymphatic hydrops in Ménière's disease: Not all that glitters is gold. *Acta Otorhinolaryngol Ital*, *38*, 369–376.
- Conte, G., Caschera, L., Calloni, S., Barozzi, S., Di Berardino, F., Zanetti, D., Scuffi, C., Scola, E., Sina, C., Triulzi, F. (2018b). MR imaging in Ménière disease: Is the contact between the vestibular endolymphatic space and the oval window a reliable biomarker? *AJNR Am J Neuroradiol*, *39*, 2114–2119.
- Counter, S. A., Bjelke, B., Klason, T., Chen, Z., Borg, E. (1999). Magnetic resonance imaging of the cochlea, spiral ganglia and eighth nerve of the guinea pig. *Neuroreport*, *10*, 473–479.
- Fraysse, B. G., Alonso, A., House, W. F. (1980). Ménière's disease and endolymphatic hydrops: Clinical-histopathological correlations. *Ann Otol Rhinol Laryngol Suppl*, *89*(6 Pt 3), 2–22.
- Holmgren, L. (1964). Hearing tests in Ménière's disease. *Acta Otolaryngol Suppl*, *192*, 115–120.
- Kobayashi, M., Yoshida, T., Sugimoto, S., Shimono, M., Teranishi, M., Naganawa, S., Sone, M. (2020). Effects of endolymphatic hydrops on acoustic energy absorbance. *Acta Otolaryngol*, *140*, 626–631.
- Lee, H. J., Jeon, J. H., Park, S., Kim, B. G., Lee, W. S., Kim, S. H. (2014). Prevalence and clinical significance of spontaneous low-frequency air-bone gaps in Ménière's disease. *Otol Neurotol*, *35*, 489–494.
- Lightfoot, G. R. (2000). Audiometer calibration: Interpreting and applying the standards. *Br J Audiol*, *34*, 311–316.
- Lopez-Escamez, J. A., & Attyé, A. (2019). Systematic review of magnetic resonance imaging for diagnosis of Meniere disease. *J Vestib Res*, *29*, 121–129.
- Lopez-Escamez, J. A., Carey, J., Chung, W. H., Goebel, J. A., Magnusson, M., Mandalà, M., Newman-Toker, D. E., Strupp, M., Suzuki, M., Trabalzini, F., Bisdorff, A.; Classification Committee of the Barany Society; Japan Society for Equilibrium Research; European Academy of Otolology and Neurotology (EAONO); Equilibrium Committee of the American Academy of Otolaryngology-Head and Neck Surgery (AAO-HNS); Korean Balance Society. (2015). Diagnostic criteria for Ménière's disease. *J Vestib Res*, *25*, 1–7.
- Muchnik, C., Hildesheimer, M., Rubinstein, M., Arenberg, I. K. (1989). Low frequency air-bone gap in Ménière's disease without middle ear pathology. A preliminary report. *Am J Otol*, *10*, 1–4.
- Naganawa, S., & Nakashima, T. (2014). Visualization of endolymphatic hydrops with MR imaging in patients with Ménière's disease and related pathologies: Current status of its methods and clinical significance. *Jpn J Radiol*, *32*, 191–204.
- Naganawa, S., Satake, H., Kawamura, M., Fukatsu, H., Sone, M., Nakashima, T. (2008a). Separate visualization of endolymphatic space, perilymphatic space and bone by a single pulse sequence; 3D-inversion recovery imaging utilizing real reconstruction after intratympanic Gd-DTPA administration at 3 Tesla. *Eur Radiol*, *18*, 920–924.
- Naganawa, S., Sugiura, M., Kawamura, M., Fukatsu, H., Sone, M., Nakashima, T. (2008b). Imaging of endolymphatic and perilymphatic fluid at 3T after intratympanic administration of gadolinium-diethylene-triamine pentaacetic acid. *AJNR Am J Neuroradiol*, *29*, 724–726.
- Naganawa, S., Yamazaki, M., Kawai, H., Bokura, K., Sone, M., Nakashima, T. (2010). Visualization of endolymphatic hydrops in

- Ménière's disease with single-dose intravenous gadolinium-based contrast media using heavily T(2)-weighted 3D-FLAIR. *Magn Reson Med Sci*, 9, 237–242.
- Naganawa, S., Kawai, H., Taoka, T., Sone, M. (2019). Improved 3D-real inversion recovery: A robust imaging technique for endolymphatic hydrops after intravenous administration of gadolinium. *Magn Reson Med Sci*, 18, 105–108.
- Nakashima, T., Naganawa, S., Sugiura, M., Teranishi, M., Sone, M., Hayashi, H., Nakata, S., Katayama, N., Ishida, I. M. (2007). Visualization of endolymphatic hydrops in patients with Meniere's disease. *Laryngoscope*, 117, 415–420.
- Nakashima T., Naganawa S., Katayama N., Teranishi M., Nakata S., Sugiura M., Sone M., Kasai S., Yoshioka M., Yamamoto M. (2009a). Clinical significance of endolymphatic imaging after intratympanic gadolinium injection. *Acta Otolaryngol Suppl*, 560, 9–14.
- Nakashima, T., Naganawa, S., Pyykko, I., Gibson, W. P., Sone, M., Nakata, S., Teranishi, M. (2009b). Grading of endolymphatic hydrops using magnetic resonance imaging. *Acta Otolaryngol Suppl*, 560, 5–8.
- Niyazov, D. M., Andrews, J. C., Strelhoff, D., Sinha, S., Lufkin, R. (2001). Diagnosis of endolymphatic hydrops *in vivo* with magnetic resonance imaging. *Otol Neurotol*, 22, 813–817.
- Okuno, T., & Sando, I. (1987). Localization, frequency, and severity of endolymphatic hydrops and the pathology of the labyrinthine membrane in Meniere's disease. *Ann Otol Rhinol Laryngol*, 96, 438–445.
- Shipton, M. S., John, A. J., Robinson, D. W. (1980). Air-radiated sound from bone vibration transducers and its implications for bone conduction audiometry. *Br J Audiol*, 14, 86–99.
- Sone, M., Naganawa, S., Teranishi, M., Nakata, S., Katayama, N., Nakashima, T. (2010). Changes in endolymphatic hydrops in a patient with Meniere's disease observed using magnetic resonance imaging. *Auris Nasus Larynx*, 37, 220–222.
- Sugimoto, S., Yoshida, T., Teranishi, M., Okazaki, Y., Naganawa, S., Sone, M. (2018). The relationship between endolymphatic hydrops in the vestibule and low-frequency air-bone gaps. *Laryngoscope*, 128, 1658–1662.
- Yetişer, S., & Kertmen, M. (2007). Cochlear conductive hearing loss in patients with Meniere's disease. *Kulak Burun Bogaz İhtis Derg*, 17, 18–21.